This article has been accepted for publication in a future issue of this journal, but has not been fully edited. Content may change prior to final publication. Citation information: DOI 10.1109/TCNS.2017.2655731, IEEE Transactions on Control of Network Systems

Centrality Measures in Linear Consensus Networks with Structured Network Uncertainties

Milad Siami† Sadegh Bolouki‡ Bassam Bamieh⋆ Nader Motee†

***Abstract*—We propose new insights into the network centrality based not only on the network graph, but also on a more structured model of network uncertainties. The focus of this paper is on the class of uncertain linear consensus networks in continuous time, where the network uncertainty is modeled by structured additive Gaussian white noise input on the update dynamics of each agent. The performance of the network is measured by the expected dispersion of its states in steady-state. This measure is equal to the square of the $\mathcal{H}_2$-norm of the network and it quantifies the extent by which its state deviates away from the consensus state in steady-state. We show that this performance measure can be explicitly expressed as a function of the Laplacian matrix of the network and the covariance matrix of the noise input. We investigate several structures for noise input and provide engineering insights on how each uncertainty structure can be relevant in real-world settings. Then, a new centrality index is defined in order to assess the influence of each agent or link on the network performance. For each noise structure, the value of the centrality index is calculated explicitly and it is shown that how it depends on the network topology as well as the noise structure. Our results assert that agents or links can be ranked according to this centrality index and their rank can drastically change from the lowest to the highest, or vice versa, depending on the noise structure. This fact hints at emergence of fundamental tradeoffs on network centrality in presence of multiple concurrent network uncertainties with different structures.**

I. Introduction

The notion of centrality in the context of complex networks determines the importance of each element within a network [1]–[10]. There are numerous ways to characterize the notion of importance in a dynamical network. One possible way is first to adopt a suitable performance index for the entire network and then quantify influence of each individual element in the network on the performance index. This view naturally leads to definition of a centrality index and an ordered ranking of elements (e.g., agents and links) by their importance. Depending on the choice of performance index, one can end up with different centrality indices [1], [2].

There are several studies in the literature that aim at defining network centrality measures based on network graphs. The node degree centrality measure is one of the popular centrality measures in the context of social networks [11], [12], where nodes with higher degrees in the network graph are of greater importance. Another context in which the degree centrality has found applications is scientific research indexing, where articles with higher citations are respected to be the more influential ones. There are several other widely used centrality indices, including eigenvector centrality [3], Katz centrality [4], closeness centrality [5], PageRank (used by Google) [6], betweenness centrality [7], [8], percolation centrality [13], cross-clique centrality [14], Freeman centralization [11], and topological centrality [15]. A comprehensive review of centrality measures can be found in [2]. Despite the presence of a large body of work on the concept of centrality in the literature, an extension of the concept to noisy dynamical networks is sorely missing.

There are several related works in the literature that address performance and robustness issues in noisy linear consensus networks; for example see [16]–[25] and the references therein. In [18], the authors investigate the deviation from the mean of states of a network on tori with additive noise inputs. The performance and robustness of networks on tori are analyzed in [16], where the effect of imperfect communication links is considered. A rather comprehensive performance analysis of noisy linear consensus networks with arbitrary graph topologies has been recently reported in [19]. In [24], [25], the authors consider the $\mathcal{H}_2$ performance measure for a class of consensus networks with exogenous inputs in the form of process and measurement noises. The proposed analysis method in [24], [25] applies the edge agreement protocol by considering a minimal realization of the edge interpretation system for simple unweighted coupling graphs.

In this paper, networks with linear consensus dynamics in the presence of structured additive noise inputs (as uncertainties) are considered. We consider a class of noisy consensus networks that can be completely characterized by their coupling graphs and the structure of their noise inputs. The $\mathcal{H}_2$-norm square of the noisy network is used as the performance measure– we refer to [16], [18], [26]–[30] for related discussions. Motivated by realistic uncertain operational environment for a network with consensus dynamics (e.g., see [31]), six noise structures are investigated in this work. Uncertainties can arise from noisy dynamics, sensors, emitters, receivers, communication channels, and measurements. To the best of our knowledge, with an exception of the dynamics noise, the comprehensive analysis of performance measures with closed-form formulae for different types of noise for an arbitrary weighted graph has not been carried out previously in the literature. Our results show that the impact of all these uncertainties can be

This research is supported by NSF-ECCS-1202517, AFOSR-YIP FA9550-13-1-0158, ONR N00014-13-1-0636, and NSF CAREER ECCS-1454022.

† M. Siami and N. Motee are with the Department of Mechanics and Mechanical Engineering, Lehigh University, Bethlehem, PA, 18015, USA e-mail: {siami, motee}@lehigh.edu.

‡ S. Bolouki is with the Coordinated Science Laboratory at the University of Illinois at Urbana-Champaign, IL 61801, USA e-mail: bolouki@uiuc.edu.

⋆B. Bamieh is with the Department of Mechanical Engineering, University of California, Santa Barbara, California 93106, USA e-mail: bamieh@engineering.ucsb.edu.

This article has been accepted for publication in a future issue of this journal, but has not been fully edited. Content may change prior to final publication. Citation information: DOI 10.1109/TCNS.2017.2655731, IEEE Transactions on Control of Network Systems

encapsulated in the structure of the input matrix. Our main contribution is the introduction of a new class of agent and link centrality indices with respect to the adopted performance measure. The key idea is to measure the infinitesimal change in the value of the performance measure with respect to the variance of the noise input. For all of the six noise structures, we calculate explicit formulae for the centrality indices and show how they depend on the topology of the coupling graph of the network. In Section VI, we discuss that for each noise structure all agents or links can be ranked in ascending order according to the value of the corresponding centrality index. As a result, every node has four different rankings and each link has two different rankings. It is argued that modification of the underlying coupling graph of the network (for example by rewiring, weight adjustment, sparsification, and adding new links) may result in emergence of fundamental tradeoffs among these rankings. Several supporting numerical simulations are shown in Section VII to illustrate the key point that centrality rank of an agent or link may significantly be different with respect to various noise structures.

II. Preliminaries

Throughout the paper, n is the number of agents and $\mathcal{V} = \{1, \ldots, n\}$ is the set of agents. The continuous time index is denoted by t. Capital letters, such as A and B refer to real-valued matrices. The transposition, Moore-Penrose pseudo-inverse, and trace of a matrix A are denoted by $A^{\rm T}$, $A^{\dagger}$, and $\mathrm{tr}(A)$, respectively. Matrices $I_n \in \mathbb{R}^{n\times n}$ and $J_n \in \mathbb{R}^{n\times n}$ are the identity matrix and the matrix of all ones, respectively. The centering matrix of size n is defined by

$$M_n \ := \ I_n - \frac{1}{n} J_n.$$

A graph can be represented by a triplet $\mathcal{G} = (\mathcal{V}, \mathcal{E}, w)$, where each agent is represented by a node, $\mathcal{E} \subseteq \{\{i,j\} \mid i,j \in \mathcal{V},\ i \neq j\}$ is the set of edges, and $w : \mathcal{E} \to (0, +\infty)$ is the weight function. The degree of each node $i \in \mathcal{V}$ is defined by

$$d_i \ := \sum_{e=\{i,j\}\in\mathcal{E}} w(e). \tag{1}$$

The adjacency matrix $A = [a_{ij}]$ of graph $\mathcal{G}$ is defined by setting $a_{ij} = w(e)$ if $e = \{i,j\} \in \mathcal{E}$, and $a_{ij} = 0$ otherwise. The Laplacian matrix of $\mathcal{G}$ is defined by

$$L := \Delta - A,$$

where $\Delta = \mathrm{diag}([d_1 \ \cdots \ d_n])$ is the degree matrix of $\mathcal{G}$. Assuming that $\{e_1, \ldots, e_m\}$ is the link set of the graph $\mathcal{G}$, we denote by E an n-by-m oriented incidence matrix of $\mathcal{G}$ defined as the following: given an arbitrary direction for all the links of $\mathcal{G}$, $E_{ik} = 1$ if the node i is the head end of the link e_k, $E_{ik} = -1$ if the node i is the tail end of the link e_k, and $E_{ik} = 0$ if the link e_k is not attached to the node i (for any orientation of links of the graph). Moreover, W is the m-by-m diagonal matrix with diagonal elements $W_{kk} = w(e_k)$ for every k, $1 \leq k \leq m$. We note that

$$L \ = \ EWE^{\rm T}.$$

Assumption 1: All graphs considered in this paper are assumed to be undirected, simple, and connected. The set of Laplacian matrices of all such graphs on n nodes are denoted by $\mathfrak{L}_n$.

The Moore-Penrose pseudo-inverse of L, denoted by $L^{\dagger}$, is a square, symmetric, doubly-centered, positive semidefinite matrix [32]. The *effective resistance* between nodes i and j is defined by:

$$r_{ij} \ := \ l_{ii}^{\dagger} + l_{jj}^{\dagger} - l_{ji}^{\dagger} - l_{ij}^{\dagger}. \tag{2}$$

A sensible interpretation of this notion is to think of effective resistance r_{ij} as the electrical resistance measured between the nodes i and j when the graph represents an electrical circuit with branch conductances given by the corresponding link weights. The white Gaussian noise with zero mean and variance σ^2 is represented by $\xi \sim N(0, \sigma^2)$.

III. Noisy Linear Consensus Networks

Consider a network of n agents with set of agents $\mathcal{V}$. Assume that each agent $i \in \mathcal{V}$ has scalar state variable $x_i(t)$ at time $t \geq 0$. The governing dynamics of linear time-invariant averaging algorithm in continuous-time is given by

$$\dot{x}_i(t) \ = \ \sum_{j\neq i} a_{ij}\left(x_j(t) - x_i(t)\right), \tag{3}$$

where all coefficient a_{ij}'s are assumed to be nonnegative. Assuming symmetric communications, i.e, $a_{ij} = a_{ji}$ for every $i, j \in \mathcal{V}$, we refer to a_{ij} as the coupling weight between agents i and j.

By imposing $a_{ii} = 0$ for all $i \in \mathcal{V}$, matrix $A = [a_{ij}]$ can be viewed as the adjacency matrix of a weighted undirected and simple graph herein called the network coupling graph and denoted by $\mathcal{G}$. The system (3) can be rewritten in the following compact form

$$\dot{x}(t) \ = \ -Lx(t), \tag{4}$$

where $x = [x_1 \ \cdots \ x_n]^{\rm T}$ is the state vector. Consensus is said to occur if for some fixed $c \in \mathbb{R}$ we have

$$\lim_{t\to\infty} x(t) \ = \ c\mathbf{1}_n,$$

where $\mathbf{1}_n \in \mathbb{R}^n$ is the vector of all ones. According to Assumption 1, the dynamics (4) achieves consensus [33], [34]. We now consider network dynamics (4) in presence of structured noise

$$\dot{x}(t) \ = \ -Lx(t) \ + \ B\xi(t), \tag{5}$$

where $L \in \mathfrak{L}_n$, and $\xi(t)$ is the vector of stochastic disturbance inputs.

Assumption 2: All components of the vector of noise input $\xi(t)$ are assumed to be independent of each other for all $t \geq 0$.

Each component of $\xi(t)$ for all $t \geq 0$ is assumed to be a white Gaussian noise with zero mean and a known variance. The input matrix B captures the noise structure in the network. The dimension and structure of matrix B may vary depending on the location of noise sources in the network. In the rest of this paper, we will refer to this matrix as the noise structure matrix. Keeping in mind that reaching consensus is what is sought in a consensus network, deviation from consensus in steady-state can be viewed as a viable performance measure for (4) that can be quantified as follows

$$\rho_{\text{ss}} \;:=\; \lim_{t\to\infty} \mathbb{E}\left[\big(x(t)-\bar{x}(t)\big)^{\mathrm{T}}\big(x(t)-\bar{x}(t)\big)\right], \qquad (6)$$

where

$$\bar{x}(t) \;:=\; \left(\frac{1}{n}\sum_{i=1}^{n} x_i(t)\right)\mathbf{1}_n$$

is the vector with all elements equal to the empirical mean of states. The larger values of ρ_{ss} indicate inferior performance levels. In an ideal situation where noise input is absent, ρ_{ss} is equal to zero.

Definition 1: For a noisy linear consensus network (5), suppose that $\xi_i(t) \sim N(0,\sigma_i^2)$ for all $t \geq 0$ is the noise associated with agent i with a known noise structure matrix $B \in \mathbb{R}^{n\times n}$. The centrality index of agent $i \in \mathcal{V}$ is defined by

$$\eta_i \;:=\; \frac{\partial \rho_{\text{ss}}}{\partial(\sigma_i^2)}. \qquad (7)$$

This quantity is equal to the rate at which ρ_{ss} changes with respect to the change of the variance of the white noise associated with agent i. Thus, the centrality index of an agent quantifies the effect of agent noise on the performance of the network.

Definition 2: For a noisy linear consensus network (5), suppose that $\xi_e(t) \sim N(0,\sigma_e^2)$ for all $t \geq 0$ is the noise associated with link e with variance σ_e^2 and a known noise structure matrix $B \in \mathbb{R}^{n\times m}$, where m is the total number of links in the underlying graph of the network. The centrality index ν_e of link $e \in \mathcal{E}$ is defined by

$$\nu_e \;:=\; \frac{\partial \rho_{\text{ss}}}{\partial(\sigma_e^2)}. \qquad (8)$$

This quantity is equal to the rate at which ρ_{ss} changes with respect to the change of the variance of the white noise associated with link e. Thus, the centrality index of a link measures impact of a link noise on the overall network performance.

In the rest of the paper, we calculate explicit values for the agent and link centrality indices for the class of networks (5) subject to several realistic noise structures.

Theorem 1: For a noisy linear consensus network (5), the value of the centrality indices (7) and (8) solely depend on the Laplacian matrix L and the noise structure matrix B. Moreover, the value of the performance measure ρ_{ss} is a linear function of the variance of the components of the vector of noise input. More specifically, for the centrality index (7), we have

$$\rho_{\text{ss}} = \sum_{i\in\mathcal{V}} \sigma_i^2\,\eta_i, \qquad (9)$$

where

$$\eta_i \;=\; \frac{\partial \rho_{\text{ss}}}{\partial(\sigma_i^2)} \;=\; \frac{1}{2}\left[B^{\mathrm{T}}L^{\dagger}B\right]_{ii} \quad \text{for all} \quad i\in\mathcal{V},$$

and for the centrality index (8), the following equation holds

$$\rho_{\text{ss}} = \sum_{e\in\mathcal{E}} \sigma_e^2\nu_e, \qquad (10)$$

where

$$\nu_e \;=\; \frac{\partial \rho_{\text{ss}}}{\partial(\sigma_e^2)} \;=\; \frac{1}{2}\left[B^{\mathrm{T}}L^{\dagger}B\right]_{ee} \quad \text{for all } e\in\mathcal{E}.$$

Proof: Let us first consider dynamics (5) with a general noise structure $B \in \mathbb{R}^{n\times p}$ and obtain its performance. Define $\xi_i(t) = \sigma_i\psi_i(t)$ for every $1 \leq i \leq p$ and rewrite dynamics (5) as:

$$\dot{x}(t) \;=\; -\,Lx(t) \;+\; B'\psi(t), \qquad (11)$$

where $B' = B\,\mathrm{diag}\big([\sigma_1,\ \cdots,\sigma_p]\big)$. Notice that ψ_i's are i.i.d Gaussian processes with variance 1. To simplify our analysis, we define an output y for the network with dynamics (11) as the following:

$$y(t) \;=\; x(t)-\bar{x}(t) \;=\; M_n x(t). \qquad (12)$$

Performance ρ_{ss} of the network with dynamics (11-12) is now equal to its squared $\mathcal{H}_2$-norm from input ψ to output y. It is note worthy that the unique marginally stable mode of dynamics (11-12) is not observable from the output, which results in the boundedness of the $\mathcal{H}_2$-norm. From the results of [35] on the $\mathcal{H}_2$-norm, we now conclude:

$$\rho_{\text{ss}} \;=\; \frac{1}{2\pi}\int_{-\infty}^{\infty} \mathrm{tr}\left(G^*(j\omega)G(j\omega)\right)d\omega, \qquad (13)$$

where $G(s)$ is the transfer function of system (11-12):

$$G(s) \;=\; M_n\big(sI+L\big)^{-1}B'. \qquad (14)$$

Let Λ be a diagonal matrix with eigenvalues $0 = \lambda_1 \leq \ldots \leq \lambda_n$ of L on its diameter and U be the corresponding orthonormal matrix of eigenvectors. Thus, we have $L = U\Lambda U^{\mathrm{T}}$. To calculate $G(s)$, we shall replace L and M_n in (14) using the following equations:

$$\begin{aligned} M_n &= U\mathrm{diag}\big([0\ 1\ \cdots\ 1]\big)U^{\mathrm{T}}, \\ L &= U\mathrm{diag}\big([0\ \lambda_2\ \cdots\ \lambda_n]\big)U^{\mathrm{T}}. \end{aligned}$$

Doing so, one concludes:

$$G(s) \;=\; U\mathrm{diag}\left(\left[0\ \frac{1}{s+\lambda_2}\ \cdots\ \frac{1}{s+\lambda_n}\right]\right)U^{\mathrm{T}}B'.$$

Thus, since $UU^{\mathrm{T}} = I_n$, one can write:

$$\begin{aligned} &\mathrm{tr}\left(G^*(j\omega)G(j\omega)\right) \qquad (15)\\ &= \ \mathrm{tr}\left(U\mathrm{diag}\left(\left[0\ \frac{1}{w^2+\lambda_2^2}\ \cdots\ \frac{1}{w^2+\lambda_n^2}\right]\right)U^{\mathrm{T}}B'B'^{\mathrm{T}}\right) \end{aligned}$$

On the other hand, we have that

$$\int_{-\infty}^{\infty}\frac{1}{w^2+\lambda_i^2}\,d\omega \;=\; \frac{\pi}{\lambda_i}. \qquad (16)$$

This article has been accepted for publication in a future issue of this journal, but has not been fully edited. Content may change prior to final publication. Citation information: DOI 10.1109/TCNS.2017.2655731, IEEE Transactions on Control of Network Systems

From (13), (15), and (16), one obtains:

$$\begin{aligned}\rho_{\text{ss}} &= \tfrac{1}{2\pi}\,\text{tr}\left(B'B'^{\text{T}}U\text{diag}\left(\left[0\ \tfrac{\pi}{\lambda_2}\ \cdots\ \tfrac{\pi}{\lambda_n}\right]\right)U^{\text{T}}\right)\\ &= \tfrac{1}{2}\,\text{tr}\left(B'B'^{\text{T}}L^{\dagger}\right).\end{aligned}\quad(17)$$

When $B \in \mathbb{R}^{n\times n}$, from relation (17) we have

$$\begin{aligned}\rho_{\text{ss}} &= \tfrac{1}{2}\,\text{tr}\left(B'B'^{\text{T}}L^{\dagger}\right)\\ &= \tfrac{1}{2}\,\text{tr}\left(B\text{diag}[\sigma_1^2\ \cdots\ \sigma_n^2]B^{\text{T}}L^{\dagger}\right)\\ &= \tfrac{1}{2}\,\text{tr}\left(\text{diag}[\sigma_1^2\ \cdots\ \sigma_n^2]B^{\text{T}}L^{\dagger}B\right).\end{aligned}\quad(18)$$

According to (18), it follows that

$$\eta_i \;=\; \partial\rho_{\text{ss}}/\partial(\sigma_i^2) \;=\; \frac{1}{2}\left[B^{\text{T}}L^{\dagger}B\right]_{ii}, \quad(19)$$

where the subscript $[\,.\,]_{ii}$ indicates the (i,i)th element and $i \in \mathcal{V}$. According to (19), we can rewrite (18) as follows

$$\rho_{\text{ss}} \;=\; \sum_{i\in\mathcal{V}} \sigma_i^2\,\eta_i.$$

When $B \in \mathbb{R}^{n\times m}$, in which m is the number of links, from relation (17) we have

$$\begin{aligned}\rho_{\text{ss}} &= \tfrac{1}{2}\,\text{tr}\left(B'B'^{\text{T}}L^{\dagger}\right)\\ &= \tfrac{1}{2}\,\text{tr}\left(\text{diag}[\sigma_1^2\ \cdots\ \sigma_m^2]B^{\text{T}}L^{\dagger}B\right).\end{aligned}\quad(20)$$

According to (20):

$$\nu_i \;=\; \partial\rho_{\text{ss}}/\partial(\sigma_i^2) \;=\; \frac{1}{2}\left[B^{\text{T}}L^{\dagger}B\right]_{ii}, \quad(21)$$

where the subscript $[\,.\,]_{ii}$ indicates the (i,i)th element and $i \in \mathcal{E}$. According to (21), we can rewrite (18) in the form of (10). ■

Our focus in this paper is on consensus networks with undirected underlying graphs. It is straightforward to generalize our results for strongly connected, balanced directed graphs. For the general case, however, when the state matrix is not normal, i.e., $LL^{\text{T}} \neq L^{\text{T}}L$, obtaining a succinct formula for the centrality measure seems to be more challenging. In [27], the authors proposed bounds that the $\mathcal{H}_2$-norm, as a performance measure, can be tightly bounded from below and above by some spectral functions of state and output matrices. Thus, one can obtain explicit bounds on the centrality measures. In addition, [36] shows how one can approximate a strongly connected digraph by some weighted undirected graph that inherits some specific properties of the original digraph. These results may be utilized to approximate centrality measures for directed networks.

IV. Agent Centrality Index

In this section, we consider four types of noise structures for network (5) and calculate the agent centrality index (7) for each case. These noise structures usually appear when one implements a consensus algorithm based on model (3) in noisy environments using uncertain communication channels and noisy sensors. In order to execute each update equation (3), each agent needs to operate in a noisy environment, sense its own state, transmit its own state information to its neighboring agents, and receive state information from its neighboring agents. In practical situations, all these steps involve uncertainties, where in this paper we model them by structured additive noise inputs.

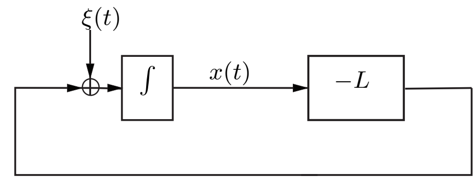

Fig. 1: A representation of linear consensus network (22) with dynamics noises.

A. Dynamics Noise

This noise structure captures the effect of environment noise on dynamics of each agent. In this case, the dynamics of agent i is described by

$$\dot{x}_i(t) \;=\; \sum_{j\neq i} a_{ij}\big(x_j(t)-x_i(t)\big) \;+\; \xi_i(t), \quad(22)$$

where $\xi_i(t) \sim N(0,\sigma_i^2)$ for all $i \in \mathcal{V}$. This class of noisy linear consensus networks has been studied before in the literature (see [18], [26]–[28] and references in there). The network dynamics (22) can be rewritten as a special case of (5) where $B = I_n$. Fig. 1 depicts a block diagram representation of linear consensus network (22) with dynamics noise. This representation is meant to illustrate the underlying mechanism of the dynamics and show how noise may affect the consensus process.

Theorem 2: For the consensus network (22) with dynamics noise, the value of the centrality index (7) can be expressed by

$$\eta_i \;=\; \frac{1}{2}\,l_{ii}^{\dagger}, \quad(23)$$

where $l_{ii}^{\dagger}$ for $i \in \mathcal{V}$ are the diagonal elements of $L^{\dagger}$.

Proof: From our arguments in Part IV-A, in case of the dynamics noise structure, one has to deal with dynamics (11)-(12) where

$$B' \;=\; \text{diag}\big([\sigma_1\ \cdots\ \sigma_n]\big).$$

We now have:

$$B'B'^{\text{T}} \;=\; \text{diag}\big([\sigma_1^2\ \cdots\ \sigma_n^2]\big). \quad(24)$$

Relation (23) now immediately follows from (17) and (24). ■

B. Receiver Noise

The communication receiver noise is the second type of noise source that can be considered in updating law (3). If agents i and j are neighbors, agent i receives $x_j(t)+\xi_i(t)$ as opposed to the clean state information $x_j(t)$, as a result of its noisy communication receiver. According to this noise model, the update equation of agent i takes the following form

$$\dot{x}_i(t) \;=\; \sum_{j\neq i} a_{ij}\big(x_j(t) - x_i(t) + \xi_i(t)\big), \tag{25}$$

where $\xi_i(t) \sim N(0, \sigma_i^2)$ for all $i \in \mathcal{V}$. The network dynamics (25) can be written as a special case of (5) where B is equal to the degree matrix $\Delta = \text{diag}([d_1 \;\cdots\; d_n])$ of the underlying coupling graph of the network.

Theorem 3: For the consensus network (25) with communication receiver noise, the value of the centrality index (7) can be calculated as

$$\eta_i \;=\; \frac{1}{2}\, d_i^2 l_{ii}^{\dagger}. \tag{26}$$

where d_i and $l_{ii}^{\dagger}$ for $i \in \mathcal{V}$ are the node degrees and the diagonal elements of $L^{\dagger}$, respectively.

Proof: Based on the description of receiver noises in Part IV-B, one has to now consider dynamics (11-12) with

$$B' \;=\; \Delta\, \text{diag}\big([\sigma_1 \;\cdots\; \sigma_n]\big), \tag{27}$$

and calculate ρ_{ss} using (17). From (27):

$$B'B'^{\mathrm{T}} \;=\; \text{diag}\big([\sigma_1^2 d_1^2 \;\cdots\; \sigma_n^2 d_n^2]\big),$$

which together with (17) result in (26). ■

C. Emitter Noise

The third type of noise source in updating law (3) can be due to the communication emitters of the neighboring agents. If agents i and j are neighbors, agent i now receives $x_j(t)+\xi_j(t)$ rather than pure state information $x_j(t)$, due to the noisy communication emitter of neighboring agent j. This noise model amounts to the following update equation for agent i:

$$\dot{x}_i(t) \;=\; \sum_{j\neq i} a_{ij}\big(x_j(t) - x_i(t) + \xi_j(t)\big), \tag{28}$$

where $\xi_i(t) \sim N(0, \sigma_i^2)$ for all $i \in \mathcal{V}$. One can reformulate the overall dynamics of the network with individual dynamics (28) and show that it is a special case of (5) with $B = A$, where A is the adjacency matrix of the underlying coupling graph of the network.

Theorem 4: For the consensus network (28) with communication emitter noise, the value of the centrality index (7) can be computed as

$$\eta_i \;=\; \frac{1}{2}\left(d_i^2 l_{ii}^{\dagger} + \left(\frac{2}{n} - 1\right) d_i\right), \tag{29}$$

where d_i and $l_{ii}^{\dagger}$ for $i \in \mathcal{V}$ are, respectively, the node degrees and the diagonal elements of $L^{\dagger}$.

Proof: From our discussion in Part IV-C, the case of emitter noises corresponds to dynamics (11-12) with

$$B' \;=\; A\, \text{diag}\big([\sigma_1 \;\cdots\; \sigma_n]\big).$$

We now have:

$$\begin{aligned} B'^{\mathrm{T}} L^{\dagger} B' \;&=\; (\Delta - L)L^{\dagger}(\Delta - L) \\ &=\; \Delta L^{\dagger}\Delta - M_n\Delta - \Delta M_n + L. \end{aligned} \tag{30}$$

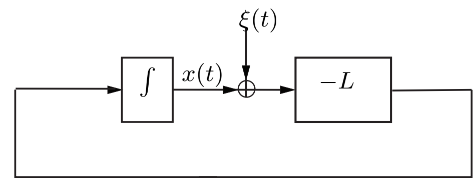

Fig. 2: A representation of linear consensus network (31) with sensor noises.

Finally, using the result of Theorem 1 and (30), we obtain the desired result (29). ■

D. Sensor Noise

The fourth type considered here is the case of noisy sensors, where each agent obtains a noisy measurement of its own current state and transmit it to the neighboring agents. The update equation of agent i can now be described by

$$\dot{x}_i(t) \;=\; \sum_{j\neq i} a_{ij}\Big[\big(x_j(t) + \xi_j(t)\big) - \big(x_i(t) + \xi_i(t)\big)\Big], \tag{31}$$

where $\xi_i(t) \sim N(0, \sigma_i^2)$ for all $i \in \mathcal{V}$. In this scenario, agent i receives $x_j(t) + \xi_j(t)$ instead of $x_j(t)$, due to the noisy sensors of its neighboring agents. On the other hand, agent i also measures a contaminated version of its own current state. The overall dynamics of the network with individual dynamics (31) can be rewritten as a special case of (5) with $B = -L$. Fig. 2 shows a representation of this linear consensus network with sensor noises.

Theorem 5: For the consensus network (31) with sensor noise, the value of the centrality index (7) can be computed as

$$\eta_i \;=\; \frac{1}{2}\, d_i, \tag{32}$$

where d_i for $i \in \mathcal{V}$ are the node degrees.

Proof: In case of sensor noises, one again deals with dynamics (11-12), but this time:

$$B' \;=\; -L\,\text{diag}\big([\sigma_1 \;\cdots\; \sigma_n]\big).$$

Thus,

$$B'B'^{\mathrm{T}} \;=\; L\text{diag}\big([\sigma_1^2 \;\cdots\; \sigma_n^2]\big)L. \tag{33}$$

From (17) and (33), we conclude:

$$\begin{aligned} \rho_{\text{ss}} \;&=\; \tfrac{1}{2}\,\text{tr}\left(L\text{diag}\left([\sigma_1^2 \;\cdots\; \sigma_n^2]\right) M_n\right) \\ &=\; \tfrac{1}{2}\,\text{tr}\left(\text{diag}\left([\sigma_1^2 \;\cdots\; \sigma_n^2]\right) L\right) \\ &=\; \tfrac{1}{2}\textstyle\sum_{i=1}^n \sigma_i^2 d_i^2. \end{aligned} \tag{34}$$

Finally, using the centrality index of an agent (7) and (34), we get the desired result. ■

Remark 1: For a connected, undirected graph with the damping factor $\alpha = 1$, PageRank is proportional to the centrality measure (32); see [37] for more details.

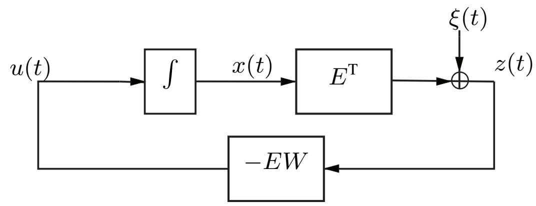

Fig. 3: A representation of linear consensus network (36-38) with communication channel noises.

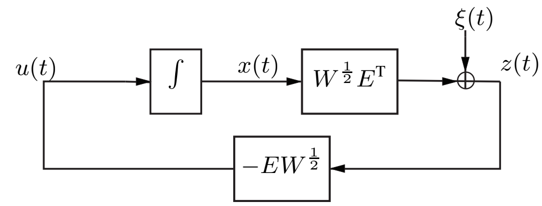

Fig. 4: A representation of linear consensus network (43-45) with measurement noises.

V. Link Centrality Index

Besides the above mentioned agent based noise inputs, there are two possible scenarios for link noises that we will consider in the following.

A. Communication Channel Noise

The first type of link noise is the communication channel noise that captures a passing signal's distortion through a communication channel between two agents in the network. This type of uncertainty can be modeled as a white Gaussian noise $\xi_e(t) \sim N(0, \sigma_e^2)$ for each $e \in \mathcal{E}$. More specifically, for an arbitrary link $e = \{i, j\} \in \mathcal{E}$, one of the endpoints of e, say i, receives $x_j(t) + \xi_e(t)$ instead of $x_j(t)$ at each time t, while the other endpoint, i.e., j, receives $x_i(t) - \xi_e(t)$ as opposed to the clean state information $x_i(t)$. Attributing a virtual orientation for e, that considers i as its head end, we derive an oriented incidence matrix E and conclude that the update algorithm of agent i can be described by

$$\dot{x}_i(t) \; = \sum_{e=\{i,j\}\in\mathcal{E}} a_{ij}\big(x_j(t) - x_i(t) + \xi_e(t)\big). \tag{35}$$

According to Assumption 2, all noises associated with distinct communication channels are independent. The overall dynamics of the network can be rewritten as a special case of (5) with $B = EW$, notice that $L = EWE^{\mathrm{T}}$. Also, in this case, we can recall the two-port representation of linear consensus network (5) as described in [25], [38] that can be cast in the following compact form

$$\dot{x}(t) \; = \; u(t), \tag{36}$$
$$z(t) \; = \; E^{\mathrm{T}}x(t) + \xi(t), \tag{37}$$

where $\xi(t) = [\ \xi_{e_1}, \ \ldots \ , \ \xi_{e_m}\ ]^{\mathrm{T}}$ is the vector of noise input, $\xi_e(t) \sim N(0, \sigma_e^2)$ for all $e \in \mathcal{E}$, and the internal feedback control law is given by

$$u(t) \; = -EWz(t), \tag{38}$$

as depicted in Fig. 3.

Theorem 6: For the consensus network (36-37) with communication channel noise, the value of the link centrality index (8) can be calculated as

$$\nu_e \; = \; \frac{1}{2}a_e^2 r_e, \tag{39}$$

where $r_e := l_{ii}^{\dagger} + l_{jj}^{\dagger} - 2l_{ij}^{\dagger}$ is the effective resistance of edge $e = \{i, j\}$ and $a_e = a_{ij}$.

Proof: Using the same approach presented in the proof of Theorem 2, we can describe the dynamics of network by (11-12) in which

$$B' \; = \; EW\,\mathrm{diag}([\sigma_1 \ \cdots \ \sigma_m]) \tag{40}$$

where E denotes the incidence matrix of underlying graph $\mathcal{G}$ and W is the diagonal matrix whose diagonal elements are respectively $w(e) = a_{ij}$ for all $e = \{i, j\} \in \mathcal{E}$. The ordering of diagonal elements in W complies with row ordering in the corresponding incident matrix E. Then, calculating the squared $\mathcal{H}_2$–norm of the network reduces to

$$\rho_{\mathrm{ss}} \; = \; \frac{1}{2}\,\mathrm{tr}\left(B'B'^{\mathrm{T}}L^{\dagger}\right). \tag{41}$$

Using (40), we get

$$B'B'^{\mathrm{T}} \; = \; E\,\mathrm{diag}([\sigma_1^2 a_{e_1}^2 \ \cdots \ \sigma_m^2 a_{e_m}^2])E^{\mathrm{T}}. \tag{42}$$

Substituting (42) into (41), we get

$$\begin{aligned} \rho_{\mathrm{ss}} \; &= \; \frac{1}{2}\,\mathrm{tr}\left(E\,\mathrm{diag}([\sigma_1^2 a_{e_1}^2 \ \cdots \ \sigma_m^2 a_{e_m}^2])E^{\mathrm{T}}L^{\dagger}\right) \\ &= \; \frac{1}{2}\,\mathrm{tr}\left(\mathrm{diag}([\sigma_1^2 a_{e_1}^2 \ \cdots \ \sigma_m^2 a_{e_m}^2])E^{\mathrm{T}}L^{\dagger}E\right) \\ &= \; \frac{1}{2}\sum_{e\in\mathcal{E}} \sigma_e^2 a_e^2 r_e. \end{aligned}$$

The last equality holds as the diagonal elements of $E^{\mathrm{T}}L^{\dagger}E$ are r_e's for $e \in \mathcal{E}$. ■

B. Measurement Noise

The second type of link noise model is used to mimic the effect of measurement noise that occurs in practice. For this case, similar to the pervious case, we can use the two-port representation of linear consensus network (5) as follows:

$$\dot{x}(t) \; = \; u(t), \tag{43}$$
$$z(t) \; = \; W^{1/2}E^{\mathrm{T}}x(t) + \xi(t), \tag{44}$$

where $\xi(t) = [\ \xi_{e_1}, \ \ldots \ , \ \xi_{e_m}\ ]^{\mathrm{T}}$ is the vector of noise input, $\xi_e(t) \sim N(0, \sigma_e^2)$ for all $e \in \mathcal{E}$, and the internal feedback control law is given by

$$u(t) \; = -EW^{1/2}z(t), \tag{45}$$

Noise structure	Centrality index η_i
Dynamics noises	$\frac{1}{2}l_{ii}^{\dagger}$
Receiver noises	$\frac{1}{2}d_i^2 l_{ii}^{\dagger}$
Emitter noises	$\frac{1}{2}\big(d_i^2 l_{ii}^{\dagger} + (\frac{2}{n} - 1)d_i\big)$
Sensor noises	$\frac{1}{2}d_i$

TABLE I: The centrality index of an agent in a noisy linear consensus network for various noise structures.

as presented in Fig. 4.

Theorem 7: For the consensus network (43-44) with measurement noise, the value of the link centrality index (8) is given by

$$\nu_e \;=\; \frac{1}{2} r_e, \tag{46}$$

where r_e is the effective resistance of edge e in the underlying graph of the network.

Proof: Using the same approach presented in the proof of Theorem 6, we can describe the dynamics of network by (11-12) in which

$$B' \;=\; E\,\mathrm{diag}\left([\sigma_1 \;\cdots\; \sigma_m]\right), \tag{47}$$

where E denotes the incidence matrix of underlying graph $\mathcal{G}$. We denote the row of E corresponds with link e by E_e, then according to the definition of effective resistance, we have

$$r_e \;=\; E_e L^{\dagger} E_e^{\mathrm{T}} \;=\; l_{ii}^{\dagger} + l_{jj}^{\dagger} - 2l_{ij}^{\dagger}, \tag{48}$$

where, $e = \{i, j\} \in \mathcal{E}$. Then, calculating the squared $\mathcal{H}_2$–norm of the network reduces to

$$\begin{aligned} \rho_{\mathrm{ss}} \;&=\; \frac{1}{2}\,\mathrm{tr}\left(B' B'^{\mathrm{T}} L^{\dagger}\right) \\ &=\; \frac{1}{2}\,\mathrm{tr}\left(E\,\mathrm{diag}([\sigma_1^2 \;\cdots\; \sigma_m^2]) E^{\mathrm{T}} L^{\dagger}\right) \\ &=\; \frac{1}{2}\,\mathrm{tr}\left(\mathrm{diag}([\sigma_1^2 \;\cdots\; \sigma_m^2]) E^{\mathrm{T}} L^{\dagger} E\right) \\ &=\; \frac{1}{2}\sum_{e\in\mathcal{E}} \sigma_e^2 r_e. \end{aligned}$$

where in the last equality we use (48). ■

Remark 2: In [15], the authors refer to quantity $1/l_{ii}^{\dagger}$ as topological centrality of node i that indicates its overall position as well as its overall connectedness in the network. This measure is closely related to the centrality index of agent i in a linear consensus network with dynamics noise (see Table I). Moreover, [15] presents three alternative interpretations for this measure in terms of: (i) detour overheads in random walks, (ii) voltage distributions and the phenomenon of recurrence when the network is treated as an electrical circuit, and (iii) the average connectedness of nodes when the network breaks into two.

VI. Centrality Rank and Inherent Tradeoffs

The results of Sections IV and V are summarized in Tables I and II. For a given noise structure, agents and links in a consensus network with dynamics (5) can be ranked according to the values of their corresponding centrality indices.

Noise structure	Centrality index ν_i
Communication noises	$\frac{1}{2}a_e^2 r_e$
Measurement noises	$\frac{1}{2}r_e$

TABLE II: The centrality index of a link for two noise structures.

Definition 3: For a given noise structure, agent $j \in \mathcal{V}$ precedes $i \in \mathcal{V}$ in rank if $\eta_i \leq \eta_j$. Similarly, link $e_2 \in \mathcal{E}$ precedes link $e_1 \in \mathcal{E}$ in rank if $\nu_{e_1} \leq \nu_{e_2}$.

Fundamental tradeoffs on centrality rank of agents and links may emerge depending on the noise structure. In the following result, we show that enhancing couplings (e.g., by strengthening link weight or establishing new links) can improve centrality of an agent or a link with respect to some noise structures and worsen it with respect to some other types.

Theorem 8: For a given agent $i \in \mathcal{V}$ and link $e \in \mathcal{E}$, suppose that functions $\phi_i, \psi_e, \delta_i : \mathfrak{L}_n \to \mathbb{R}$ are defined by $\phi_i(L) = l_{ii}^{\dagger}$, $\psi_e(L) = r_e$, and $\delta_i(L) = d_i$. Then, functions ϕ_i and ψ_e are monotonically decreasing and function δ_i is monotonically increasing as a function of L, i.e., for all $L_1 \preceq L_2$ it follows that

$$\begin{aligned} \phi_i(L_2) \;&\leq\; \phi_i(L_1), & (49)\\ \psi_e(L_2) \;&\leq\; \psi_e(L_1), & (50)\\ \delta_i(L_1) \;&\leq\; \delta_i(L_2). & (51) \end{aligned}$$

Proof: Let us consider the real-valued function $f(L, Q) = \mathrm{tr}(QL)$. From matrix calculus, one gets

$$\frac{\partial f(L,Q)}{\partial L} \;=\; Q. \tag{52}$$

When $Q_i = \mathrm{diag}[0, \cdots, 1, \cdots, 0]$, i.e., a diagonal matrix with only one nonzero element on its i-th diagonal element, function f reduces to $f(L, Q_i) = \delta_i(L) = d_i$. According to (52) and the fact that $Q_i \succeq 0$, one can conclude that function $f(L, Q_i) = \delta_i(L)$ is monotonically increasing.

In the next step, let us consider the real-valued function $g(L, Q) = \mathrm{tr}(QL^{\dagger})$. A direct matrix calculation gives us

$$\frac{\partial g(L,Q)}{\partial L} \;=\; -\,L^{\dagger} Q L^{\dagger}. \tag{53}$$

The function $g(L, Q_i)$ is equal to $l_{ii}^{\dagger}$. Therefore, $\phi_i(L) = l_{ii}^{\dagger}$ is monotonically decreasing, because $-L^{\dagger} Q_i L^{\dagger} \preceq 0$ for all $i = 1, \ldots, n$. Furthermore, if Q_e is the Laplacian matrix of a graph with only one link $e = \{i, j\}$, then the function $g(L, Q_e)$ is equal to r_e. Using (53) and the fact that $-L^{\dagger} Q_e L^{\dagger} \preceq 0$, we can conclude that $\psi_e(L) = r_e$ is monotonically decreasing. ■

According to this theorem, by enhancing couplings one may expect to observe drastic changes in each agent's and link's ranking with respect to various noise structures. For instance, suppose that for a given consensus network agent i is ranked s_1 w.r.t. sensor noise and t_1 w.r.t. dynamics noise, where $s_1 > t_1$. It is likely that after adding new links or increasing weight

This article has been accepted for publication in a future issue of this journal, but has not been fully edited. Content may change prior to final publication. Citation information: DOI 10.1109/TCNS.2017.2655731, IEEE Transactions on Control of Network Systems

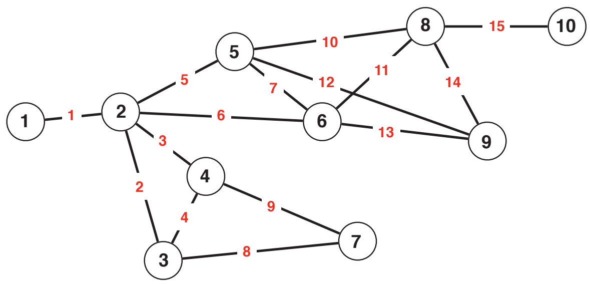

Fig. 5: The network topology for Example 1. The red labels on the links represent link numbers.

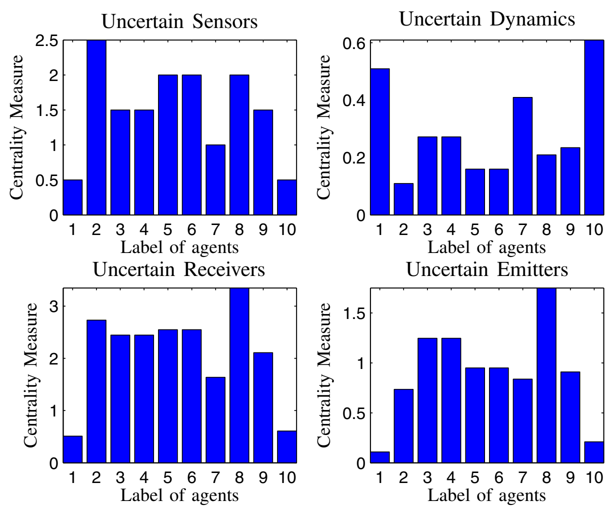

Fig. 6: The agent centrality indices for different noise structures and the coupling graph of Fig. 5.

links, the same agent i gets ranked s_2 w.r.t. sensor noise and t_2 w.r.t. dynamics noise, but this time $t_2 > s_2$. This key point is explained in details using several numerical simulations in the following section.

The result of Theorem 8 can be leveraged further to identify inherent performance tradeoffs due to direction of monotonicity for different types of uncertainties. From the result of Theorem 1, the value of performance measure can be equivalently characterized with respect to various centrality measures as follows

$$\begin{aligned} \rho_{ss} &= \frac{1}{2}\sum_{i\in\mathcal{V}} \sigma_i^2 \phi_i(L) \\ &= \frac{1}{2}\sum_{i\in\mathcal{V}} \sigma_i^2 \delta_i(L) \end{aligned}$$

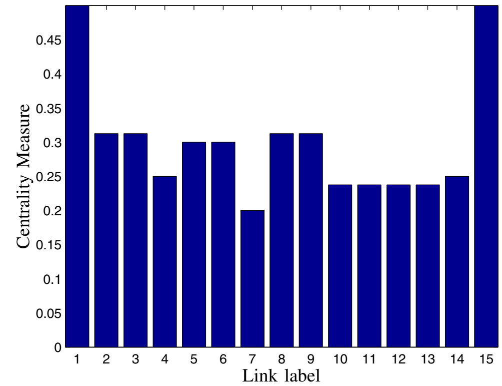

Fig. 7: The link centrality indices for the coupling graph of Fig. 5. Since the coupling graph is unweighted, both proposed link centrality indices in Table II are identical.

$$= \frac{1}{2}\sum_{e\in\mathcal{E}} \sigma_e^2 \psi_e(L),$$

Therefore, according to Theorem 8, if $L_1 \preceq L_2$, we can conclude that in presence of dynamics and sensor noises the performance of network 2 is not worse than the performance of network 1, whereas in presence of measurement noise the performance of network 2 is not better than the performance of network 1. For a given network with Laplacian matrix L_1, inequality $L_1 \preceq L_2$ can be realized via several possible scenarios; for example, network 2 can be constructed by (i) adding new weighted edges to the graph of network 1, (ii) increasing weights of some of the existing links in network 1, (iii) rewiring topology of network 1 while ensuring $L_1 \preceq L_2$. The final conclusion is that strengthening couplings among the agents may improve or deteriorate the performance depending on the noise structure.

VII. Illustrative Numerical Examples

In this section, we support our theoretical results by illustrating several examples to provide better insight about agent and link centrality measures in noisy linear consensus networks.

Example 1: Let us consider a noisy linear consensus network with coupling graph shown in Fig. 5. It is assumed that every link has weight 1. For this network, the centrality index of all 10 agents are calculated for different noise structures according to Table I and are depicted in Fig. 6. One observes that while agents 1 and 10 are the *most central* agents w.r.t. dynamics noise, they are the *least central* w.r.t. the other remaining three noise structures. According to Fig. 6 for uncertain sensors, one can rank all agents based on their corresponding node degrees, which can be easily deduced from the graph topology. However, we observe that in presence of dynamics, receiver, and emitter noises there is no trivial way to relate topology of the underlying coupling graph of the network to agents' centrality rank. For the same network, the links are ranked according to Table II and the result is

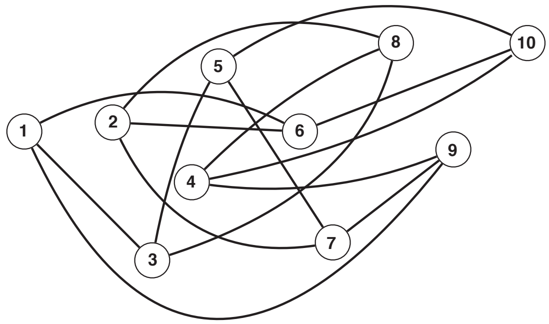

Fig. 8: The network topology for Example 2.

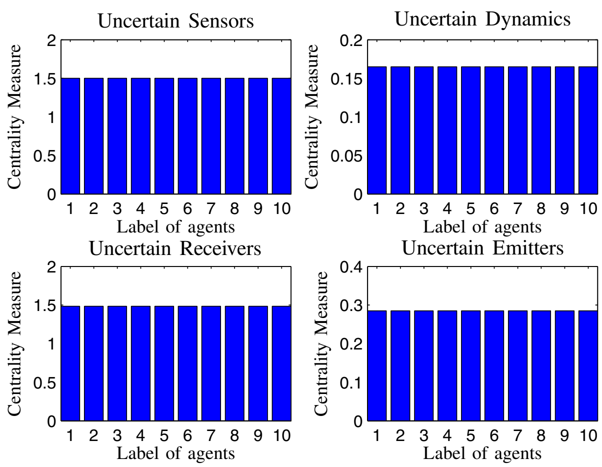

Fig. 9: The centrality indices of all agents for a noisy linear consensus network defined by the coupling graph in Fig. 8.

depicted in Fig. 7. Since the underlying graph is unweighted, both centrality measures in Table II are the same. One observes that links number 1 and 15 are the most central links. This is compatible with the fact that by eliminating any of these two links the underlying graph becomes disconnected.

Example 2: We simulate a noisy linear consensus network with coupling graph shown in Fig. 8, where it is assumed that all link weights are equal to 1. This graph is indeed a rewired form of the graph in Fig. 5 – both graphs share the same number of nodes and links. The agent centrality indices are drawn according to Table I in Fig. 9. It can be seen that all agents have equal ranks (i.e., importance) in the network for all four noise structures. The link centrality indices are depicted in Fig. 10, where it is shown that all links have equal ranks. These observations are consistent with our results and can be explained as follows: since the coupling graph in Fig. 8 is symmetric (i.e., link-transitive and node-transitive) and unweighted, all nodes and links contribute equally to the performance of the network.

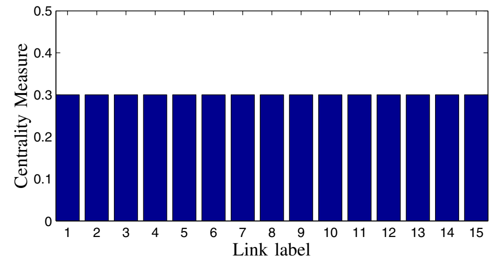

Fig. 10: Links' centrality for the coupling graph of Fig. 8. Since, the coupling graph is unweighted both link centrality measures in Table II are the same.

Example 3: In our last simulation, we study link centrality rank for a noisy linear consensus network with coupling graph in Fig. 11, where this graph consists of 108 links and three groups of 10 agents that each group is shown by red, green, and blue colors. We calculate link centrality indices according to Table II for several scenarios. In Fig. 12, the link centrality indices are depicted when it is assumed that all links in the graph have weights equal to 1, except for $w(\mathrm{A}) = w(\mathrm{B}) = w(\mathrm{C}) = w(\mathrm{D}) = 0.2$. One observes that the intergroup links $\mathrm{A}, \mathrm{B}, \mathrm{C}$, and D are significantly more important than the intragroup links. Both links A and B are the most central ones as without them the network graph will be disconnected.

The link centrality index of an edge with respect to measurement noise is proportional to the effective resistance of that link from our results in Table II. The result of Theorem 8 asserts that by increasing weights of links A, B, C, and D, their centrality rank will drop accordingly. This can be clearly seen in our simulations in Figures 12, 13, 14, and 15, where the weights of these four links are increased from 0.2 to 1, then to 3, and finally to 10. These four links, however, remain the most central links with respect to communication noises and their roles do not change by changing their weights.

VIII. Conclusion

A new definition of centrality, with respect to the $\mathcal{H}_2$-norm square, is introduced for networks with consensus dynamics subject to structured additive noise inputs. In such networks, the centrality of each agent or link depends on the underlying coupling graph of the network as well as the structure of noise input. We model several noise structures based on realistic operational situations. It is shown that the centrality index of agents and links solely depends on the characteristics of the underlying coupling graph. We discuss that the centrality rank of agents or links may vary substantially when comparing various noise structures. More importantly, it is argued that when one modifies the coupling graph of the network (for instance by rewiring, weight adjustment, sparsification, and adding new links), the agent and link centrality ranks may drastically shift up or down in the list. Since in real-world situations there are several possible sources of uncertainties

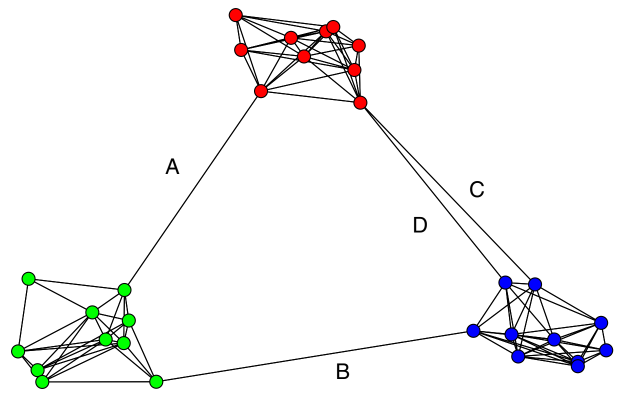

Fig. 11: The network topology for Example 3.

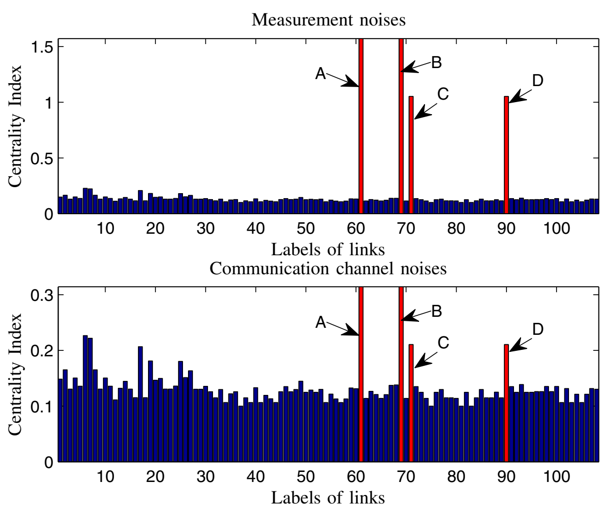

Fig. 12: The link centrality indices for the consensus network with graph topology Fig. 11. It is assumed that all link weights are equal to 1, except for $w(\mathrm{A}) = w(\mathrm{B}) = w(\mathrm{C}) = w(\mathrm{D}) = 0.2$. The centrality indices of links $\mathrm{A}, \mathrm{B}, \mathrm{C}$, and D are shown by red bars.

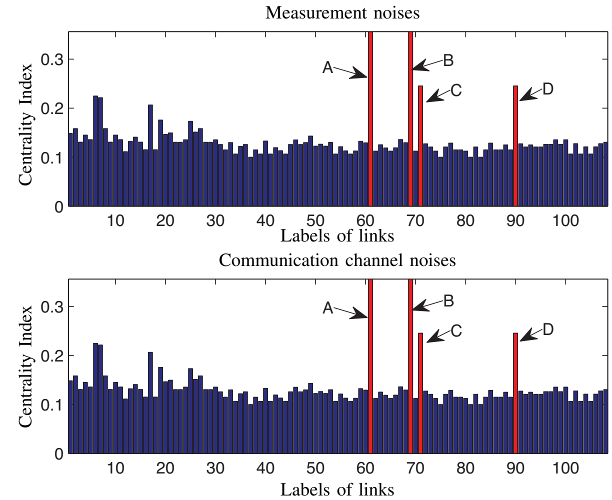

Fig. 13: The link centrality indices for the consensus network with graph topology Fig. 11, where all link weights are equal to 1. In this plot A, B, C, and D are labels of links between three clusters. The centrality indices of links $\mathrm{A}, \mathrm{B}, \mathrm{C}$, and D are shown by red bars.

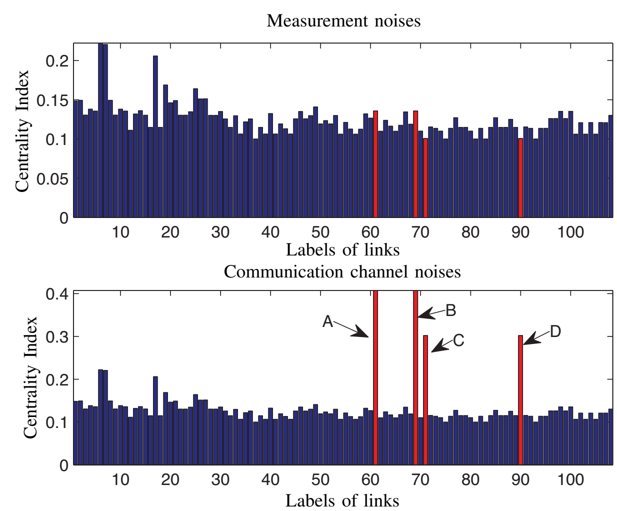

Fig. 14: The link centrality indices for the consensus network with graph topology Fig. 11. It is assumed that all link weights are equal to 1, except for $w(\mathrm{A}) = w(\mathrm{B}) = w(\mathrm{C}) = w(\mathrm{D}) = 3$. The centrality indices of these links $\mathrm{A}, \mathrm{B}, \mathrm{C}$, and D are shown by red bars.

that can affect the dynamics of a consensus network simultaneously, it would be a challenging task to determine the most central agents or links without taking into account the existing fundamental tradeoffs among various centrality ranks. This inherent phenomenon in uncertain consensus networks suggests revisiting and reformulating several existing canonical network optimization problems in the literature by taking into account the agent and link centrality ranks in the design process in order to synthesize more robust consensus networks.

REFERENCES

[1] M. Newman, *Networks: an introduction*. Oxford University Press, 2010.

[2] M. Benzi and C. Klymko, “On the limiting behavior of parameter-dependent network centrality measures,” *SIAM Journal on Matrix Analysis and Applications*, vol. 36, no. 2, pp. 686–706, 2015.

[3] P. Bonacich, “Power and centrality: A family of measures,” *American journal of sociology*, pp. 1170–1182, 1987.

[4] L. Katz, “A new status index derived from sociometric analysis,” *Psychometrika*, vol. 18, no. 1, pp. 39–43, 1953.

This article has been accepted for publication in a future issue of this journal, but has not been fully edited. Content may change prior to final publication. Citation information: DOI 10.1109/TCNS.2017.2655731, IEEE Transactions on Control of Network Systems

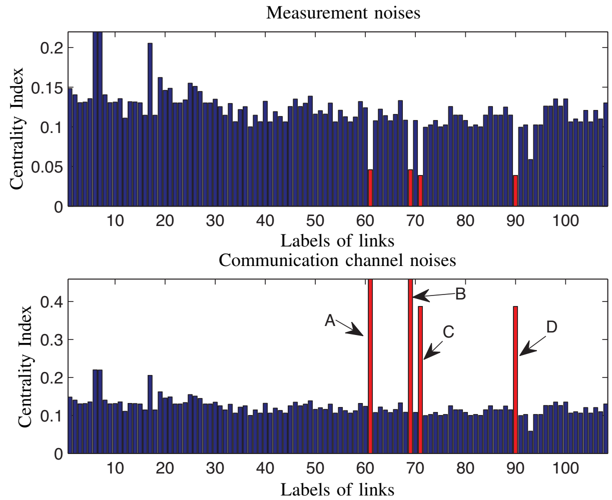

Fig. 15: The link centrality indices for the consensus network with graph topology Fig. 11. It is assumed that all link weights are equal to 1, except for $w(\mathrm{A}) = w(\mathrm{B}) = w(\mathrm{C}) = w(\mathrm{D}) = 10$. The indices of links $\mathrm{A}, \mathrm{B}, \mathrm{C}$, and D are shown by red bars.

[5] D. J. Watts and S. H. Strogatz, "Collective dynamics of "small-world" networks," *nature*, vol. 393, no. 6684, pp. 440–442, 1998.

[6] S. Brin and L. Page, "Reprint of: The anatomy of a large-scale hypertextual web search engine," *Computer networks*, vol. 56, no. 18, pp. 3825–3833, 2012.

[7] J. M. Anthonisse, "The rush in a directed graph," *Stichting Mathematisch Centrum. Mathematische Besliskunde*, no. BN 9/71, pp. 1–10, 1971.

[8] L. C. Freeman, "A set of measures of centrality based on betweenness," *Sociometry*, pp. 35–41, 1977.

[9] H. Tanner, "On the controllability of nearest neighbor interconnections," in *43rd IEEE Conference on Decision and Control*, vol. 3, pp. 2467–2472, 2004.

[10] M. R. Faghani and U. T. Nguyen, "A study of xss worm propagation and detection mechanisms in online social networks," *IEEE Transactions on Information Forensics and Security*, vol. 8, no. 11, pp. 1815–1826, 2013.

[11] L. C. Freeman, "Centrality in social networks conceptual clarification," *Social networks*, vol. 1, no. 3, pp. 215–239, 1972.

[12] P. Bonacich, "Factoring and weighting approaches to status scores and clique identification," *Journal of Mathematical Sociology*, vol. 2, no. 1, pp. 113–120, 1972.

[13] L. H. M. Piraveenan, M. Prokopenko, "Percolation centrality: Quantifying graph-theoretic impact of nodes during percolation in networks," *PLoS ONE*, vol. 8, no. 1, pp. 1789–1802, 2013.

[14] M. G. Everett and S. P. Borgatti, "Analyzing clique overlap," *Connections*, vol. 21, no. 1, pp. 49–61, 1998.

[15] G. Ranjan and Z.-L. Zhang, "Geometry of complex networks and topological centrality," *Physica A: Statistical Mechanics and its Applications*, vol. 392, no. 17, pp. 3833–3845, 2013.

[16] N. Elia, J. Wang, and X. Ma, "Mean square limitations of spatially invariant networked systems," in *Control of Cyber-Physical Systems* (D. C. Tarraf, ed.), vol. 449 of *Lecture Notes in Control and Information Sciences*, pp. 357–378, Springer International Publishing, 2013.

[17] G. F. Young, L. Scardovi, and N. E. Leonard, "Robustness of noisy consensus dynamics with directed communication," in *2010 American Control Conference*, pp. 6312–6317, July 2010.

[18] B. Bamieh, M. Jovanović, P. Mitra, and S. Patterson, "Coherence in large-scale networks: Dimension-dependent limitations of local feedback," *IEEE Transactions on Automatic Control*, vol. 57, no. 9, pp. 2235 –2249, 2012.

[19] M. Siami and N. Motee, "Fundamental limits and tradeoffs on disturbance propagation in linear dynamical networks," *IEEE Transactions on Automatic Control*, vol. 61, pp. 4055–4062, Dec 2016.

[20] R. Carli, F. Fagnani, P. Frasca, T. Taylor, and S. Zampieri, "Average consensus on networks with transmission noise or quantization," in *2007 European Control Conference*, pp. 1852–1857, 2007.

[21] A. Sahai and S. Mitter, "The necessity and sufficiency of anytime capacity for stabilization of a linear system over a noisy communication link," *IEEE Transactions on Information Theory*, vol. 52, no. 8, pp. 3369–3395, 2006.

[22] F. Fagnani and S. Zampieri, "Average consensus with packet drop communication," *SIAM Journal on Control and Optimization*, vol. 48, no. 1, pp. 102–133, 2009.

[23] M. Huang and J. H. Manton, "Coordination and consensus of networked agents with noisy measurements: Stochastic algorithms and asymptotic behavior," *SIAM Journal on Control and Optimization*, vol. 48, no. 1, pp. 134–161, 2009.

[24] D. Zelazo, S. Schuler, and F. Allgöwer, "Performance and design of cycles in consensus networks," *Systems & Control Letters*, vol. 62, no. 1, pp. 85–96, 2013.

[25] D. Zelazo and M. Mesbahi, "Edge agreement: Graph-theoretic performance bounds and passivity analysis," *IEEE Transactions on Automatic Control*, vol. 56, no. 3, pp. 544–555, 2011.

[26] A. Jadbabaie and A. Olshevsky., "Combinatorial bounds and scaling laws for noise amplification in networks," in *2013 European Control Conference*, pp. 596–601, July 2013.

[27] M. Siami and N. Motee, "Robustness and performance analysis of cyclic interconnected dynamical networks," in *2013 SIAM Conference on Control and Its Application*, pp. 137–143, Jan. 2013.

[28] M. Siami and N. Motee, "Fundamental limits on robustness measures in networks of interconnected systems," in *52nd IEEE Conference on Decision and Control*, pp. 67–72, Dec. 2013.

[29] K. Fitch and N. Leonard, "Information centrality and optimal leader selection in noisy networks," in *52nd IEEE Conference on Decision and Control*, pp. 7510–7515, 2013.

[30] F. Lin, M. Fardad, and M. R. Jovanović, "Algorithms for leader selection in stochastically forced consensus networks," *IEEE Transactions on Automatic Control*, vol. 59, no. 7, pp. 1789–1802, 2014.

[31] L. F. Bertuccelli, H. Choi, P. Cho, and J. P. How, "Real-time multi-uav task assignment in dynamic and uncertain environments," in *AIAA Guidance, Navigation, and Control Conference*, 2009.

[32] I. Gutman and W. Xiao, "Generalized inverse of the laplacian matrix and some applications," *Bulletin: Classe des Sciences Mathématiques et Naturelles. Sciences Mathématiques*, vol. 129, no. 29, pp. 15–23, 2004.

[33] W. Ren, R. W. Beard, and T. W. McLain, "Coordination variables and consensus building in multiple vehicle systems," in *Cooperative Control*, pp. 171–188, Springer, 2005.

[34] Z. Lin, B. Francis, and M. Maggiore, "Necessary and sufficient graphical conditions for formation control of unicycles," *IEEE Transactions on Automatic Control*, vol. 50, no. 1, pp. 121–127, 2005.

[35] J. Doyle, K. Glover, P. Khargonekar, and B. Francis, "State-space solutions to standard $\mathcal{H}_2$ and $\mathcal{H}_\infty$ control problems," *IEEE Transactions on Automatic Control*, vol. 34, no. 8, pp. 831–847, 1989.

[36] D. Boley, G. Ranjan, and Z.-L. Zhang, "Commute times for a directed graph using an asymmetric laplacian," *Linear Algebra and its Applications*, vol. 435, no. 2, pp. 224 – 242, 2011.

[37] D. F. Gleich, "Pagerank beyond the web," *SIAM Review*, vol. 57, no. 3, pp. 321–363, 2015.

[38] M. Siami and N. Motee, "Performance analysis of linear consensus networks with structured stochastic disturbance inputs," in *2015 American Control Conference*, pp. 4080–4085, 2015.

This article has been accepted for publication in a future issue of this journal, but has not been fully edited. Content may change prior to final publication. Citation information: DOI 10.1109/TCNS.2017.2655731, IEEE Transactions on Control of Network Systems

Milad Siami received his dual B.Sc. degrees in electrical engineering and pure mathematics from Sharif University of Technology in 2009, M.Sc. degree in electrical engineering from Sharif University of Technology in 2011, M.Sc. and Ph.D. degrees in mechanical engineering from Lehigh University in 2014 and 2016. From 2009 to 2010, he was a research student at the Department of Mechanical and Environmental Informatics at the Tokyo Institute of Technology, Tokyo, Japan. His research interests include distributed control systems, distributed optimization, and applications of fractional calculus in engineering. He received a Gold Medal of National Mathematics Olympiad, Iran (2003) and the Best Student Paper Award at the 5th IFAC Workshop on Distributed Estimation and Control in Networked Systems (2015). Moreover, he was awarded RCEAS Fellowship (2012), Byllesby Fellowship (2013), Rossin College Doctoral Fellowship (2015), and Graduate Student Merit Award (2016) at Lehigh University.

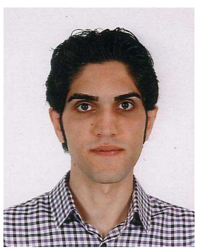

Sadegh Bolouki received the B.S. and Ph.D. degrees in Electrical Engineering from Sharif University of Technology and cole Polytechnique de Montral in 2008 and 2014, respectively. From January 2014 to July 2015, he was a research associate at the Department of Mechanical Engineering and Mechanics at Lehigh University. Since August 2015, he has been a postdoctoral research associate at the Coordinated Science Lab at the University of Illinois, Urbana-Champaign. His research interests include the areas of Distributed Systems, Complex Networks, Game Theory, Fractional Calculus, and Chaos Theory.

Bassam Bamieh (M'90-SM'02-F'08) is Professor of Mechanical Engineering and Associate Director of the Center for Control, Dynamical Systems and Computation at the University of California at Santa Barbara (UCSB). He received his B.Sc. degree in Electrical Engineering and Physics from Valparaiso University (Valparaiso, IN) in 1983, and his M.Sc. and PhD degrees in Electrical and Computer Engineering from Rice University (Houston, TX) in 1986 and 1992 respectively. Prior to joining UCSB in 1998, he was an Assistant Professor in the Department of Electrical and Computer Engineering and the Coordinated Science Laboratory at the University of Illinois at Urbana-Champaign (1991-98). His research interests are in robust and optimal control, spatially distributed systems, and problems at the interface between controls, fluid mechanics and statistical physics. He is a past recipient of the IEEE Control Systems Society G. S. Axelby Outstanding Paper Award (twice), the AACC Hugo Schuck Best Paper Award, and a National Science Foundation CAREER award. He is a Fellow of the International Federation of Automatic Control (IFAC), and a Fellow of the IEEE.

Nader Motee (S'99-M'08-SM'13) received his B.Sc. degree in Electrical Engineering from Sharif University of Technology in 2000, M.Sc. and Ph.D. degrees from University of Pennsylvania in Electrical and Systems Engineering in 2006 and 2007 respectively. From 2008 to 2011, he was a postdoctoral scholar in the Control and Dynamical Systems Department at Caltech. Since 2011, he has been the P.C. Rossin Assistant Professor in the Department of Mechanical Engineering and Mechanics at Lehigh University. His current research area is distributed dynamical and control systems with particular focus on issues related to sparsity, performance, and robustness. He is a past recipient of several awards including the 2008 AACC Hugo Schuck best paper award, the 2007 ACC best student paper award, the 2008 Joseph and Rosaline Wolf best thesis award, a 2013 Air Force Office of Scientific Research Young Investigator Program award (AFOSR YIP), a 2015 NSF Faculty Early Career Development (CAREER) award, and a 2016 Office of Naval Research Young Investigator Program award (ONR YIP).